Geochemical Perspectives Letters

Contrasting controls on $\delta^{18}O$-$\delta^{2}H$ and $\delta^{18}O$-$\delta^{17}O$ systematics in a balance filled lake

M.J. Custado[1,2*], A.R. Waldeck[1,3], B. Belanger[4], X.-K. Wang[1], J.C.K. Rugenstein[5], K.M. Cobb[1,2], J.L. Oster[4], D.E. Ibarra[1,2]

Abstract

https://doi.org/10.7185/geochemlet.2631

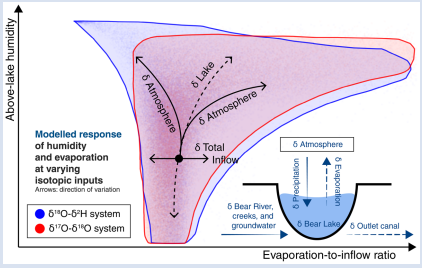

Recent analytical advancements now allow precise quantification of ^{17}O excess ($\Delta'^{17}O$), introducing the triple oxygen isotope system ($\delta^{17}O$-$\delta^{18}O$) as a complementary tool to d-excess, its analogue in the classic $\delta^{18}O$-$\delta^{2}H$ system. Therefore, the objective of this study is to contrast the sensitivities of the $\delta^{18}O$-$\delta^{2}H$ and $\delta^{18}O$-$\delta^{17}O$ systems to varying environmental and isotopic parameters. To do this, we present a new triple oxygen isotope data set from the Bear River watershed (Utah/Idaho, USA) and model lake evaporation trajectories using Monte Carlo driven steady state mass balance modelling. Results demonstrate that $\Delta'^{17}O$ provides more accurate humidity constraints. Modelling the evaporation trajectories of the balance filled Bear Lake, we show that the uncertainty of the calculated lake isotopic composition increases with increasing evaporation-to-inflow ratio (X_e). This observation implies the need to better constrain isotopic inputs, particularly that of atmospheric moisture, in dry environments where X_e is high. Further, this study highlights the need for a larger $\Delta'^{17}O$ data set aggregation across environmental conditions to better characterise variability and reduce uncertainty in calibrating isotope mass balance models.

Received 1 March 2026 | Accepted 3 August 2026 | Published 8 September 2026

Introduction

Stable isotope hydrology in lakes has traditionally relied on $\delta^{18}O$-$\delta^{2}H$ systematics to constrain lake water balance (Gonfiantini, 1986; Gat, 1995; Gibson *et al.*, 2016). Initially, $\delta^{17}O$ was believed to provide no additional information beyond the $\delta^{18}O$-$\delta^{2}H$ framework. However, analytical advancements now allow the precise quantification of mass dependent fractionation between $\delta^{17}O$ and $\delta^{18}O$, from which an analogue to d-excess, ^{17}O excess ($\Delta'^{17}O$), can be calculated. Previous studies have noted the relative insensitivity of $\Delta'^{17}O$ to temperature compared to d-excess (Angert *et al.*, 2004; Uemura *et al.*, 2010). This characteristic increases the potential of the $\delta^{17}O$-$\delta^{18}O$ system to provide unique hydrological information in both modern (Pierchala *et al.*, 2022; Voigt *et al.*, 2025) and palaeoclimate settings, where it has been used to reconstruct humidity and evaporation conditions (Gázquez *et al.*, 2018; Passey and Ji, 2019; Gázquez-Sánchez *et al.*, 2023; Katz *et al.*, 2023). Its utility may be greatest in studies using mineral archives, particularly authigenic carbonates, where paired $\delta^{2}H$ data cannot be extracted from the same mineral. The introduction of high throughput instruments to measure $\delta^{17}O$ has further enhanced measurement efficiency and precision, supplementing existing tools for palaeoclimate research and modern water management (*e.g.*, Berman *et al.*, 2013; Steig *et al.*, 2021).

In this study, we present a new triple oxygen isotope data set from Bear Lake, Utah/Idaho to derive relative humidity and evaporation-to-inflow ratios. By comparing the triple oxygen and $\delta^{18}O$-$\delta^{2}H$ data from replicates of the same samples (*cf.* Custado *et al.*, 2025), we highlight how each system constrains key parameters, demonstrating the added utility of $\Delta'^{17}O$ in lake balance applications. This work is compared to previous $\Delta'^{17}O$ data from Bear Lake (Passey and Ji, 2019) and comparable modelling for other mid-latitude lakes (Surma *et al.*, 2015, 2018; Gázquez *et al.*, 2018; Voigt *et al.*, 2021, 2025).

Steady State Isotopic Mass Balance Equations

The Craig-Gordon evaporation model is often used to describe isotope exchange at the water-atmosphere interface during evaporation of an open water body (Craig and Gordon, 1965). The kinetic component of this isotopic process can be modelled through molecular diffusion, as predicted by kinetic theory (Criss, 1999). Building on these concepts, the following equation represents the steady state isotopic mass balance of a well mixed, throughflow lake (Craig and Gordon, 1965; Gonfiantini, 1986; Criss, 1999; Gibson *et al.*, 2016; Passey and Levin, 2021):

1. Department of Earth, Environmental, and Planetary Sciences, Brown University
2. Institute at Brown University for Environment and Society, Brown University
3. Department of Geosciences, Pennsylvania State University
4. Department of Earth and Environmental Sciences, Vanderbilt University
5. Department of Geosciences, Colorado State University

* Corresponding author (email: manuel_justin_custado@brown.edu)

$$R_L = \frac{\alpha_{eq}\alpha_{diff}(1-h)R_I + \alpha_{eq}hX_eR_A}{\alpha_{eq}\alpha_{diff}(1-h)(1-X_e) + X_e} \quad \text{Eq. 1}$$

where R represents isotopic (^{17}O, ^{18}O, ^{2}H) compositions expressed in ratios relative to a known standard (Vienna Standard Mean Ocean Water, VSMOW). The subscripts L, A, and I denote the steady state isotopic compositions of the lake, atmospheric moisture, and inflow, respectively. The variable h represents relative humidity normalised to the lake surface temperature, X_e the evaporation-to-inflow ratio, α_{eq} the equilibrium fractionation factor, and α_{diff} the kinetic fractionation at zero humidity (diffusion end member). Note that in Criss (1999), $\alpha_{eq}{\cdot}\alpha_{diff}$ is expressed as α^{0}_{evap}. This work follows the conventions for α in Gonfiantini (1986), where $\alpha > 1$.

We applied Equation 1 to both triple oxygen and $\delta^{18}O$-$\delta^{2}H$ isotope systems. Ratios are preferred in triple oxygen isotopic calculations as $\Delta'^{17}O$ is derived from linearised isotopic data (δ'; Eq. 2; Miller, 2002; Luz and Barkan, 2010):

$$\delta' = \ln(R) \quad \text{Eq. 2}$$

A full description of the equations is provided in the Supplementary Information.

Study Site

Bear Lake lies within the semi-arid northeast Great Basin, bounded by the Bear Lake Plateau and Bear River Range (Fig. 1). The lake is primarily fed by the Bear River through an inlet canal, whose headwaters are located further south in the Uinta Mountains. Surrounding creeks and springs provide additional input, particularly those originating from the Bear River Range. Groundwater is estimated to have a minor contribution (Bright, 2009; Custado *et al.*, 2025). Most precipitation falls as snow, which reaches the lake through immediate and delayed snowmelt *via* streams. Water exits the lake through evaporation and an outlet canal (Bright, 2009). Annual volumetric discharge of each inflow component is summarised in Table S-1. Additionally, a brief description of the physical and hydroclimatic setting of the lake is provided in the Supplementary Information.

Analytical and Computational Methods

Lake, stream, and groundwater samples were collected during baseflow in August 2023 (Fig. 1) and analysed along with isotopic standards using a Picarro L2140-i cavity ring down spectrometer at Brown University, USA. Precipitation samples were obtained from sampling stations located in Utah State University and Utah Valley University. Analytical drift and memory corrections were applied before data normalisation to the VSMOW-SLAP scale using internally calibrated reference waters (Gröning, 2011; Hutchings and Konecky, 2023).

The second order isotopic parameters are calculated using the following equations:

$$\Delta'^{17}O = \delta'^{17}O - 0.528 \times \delta'^{18}O \quad \text{Eq. 3}$$

$$\text{d-excess} = \delta^{2}H - 8 \times \delta^{18}O \quad \text{Eq. 4}$$

Relative humidity and X_e from each isotope system were derived using Monte Carlo simulations ($n = 100{,}000$) of Equation 1, with input distributions generated from measured isotope data of samples and corresponding analytical uncertainties (Table S-2, Fig. S-1). A detailed description of the computational approach is provided in the Supplementary Information.

Final values reported in Table 1 are the median of the output distributions (Fig. S-2), with uncertainties expressed as the interquartile range (IQR, 25th-75th percentiles). Means and standard deviations (1σ) are reported in Table S-3.

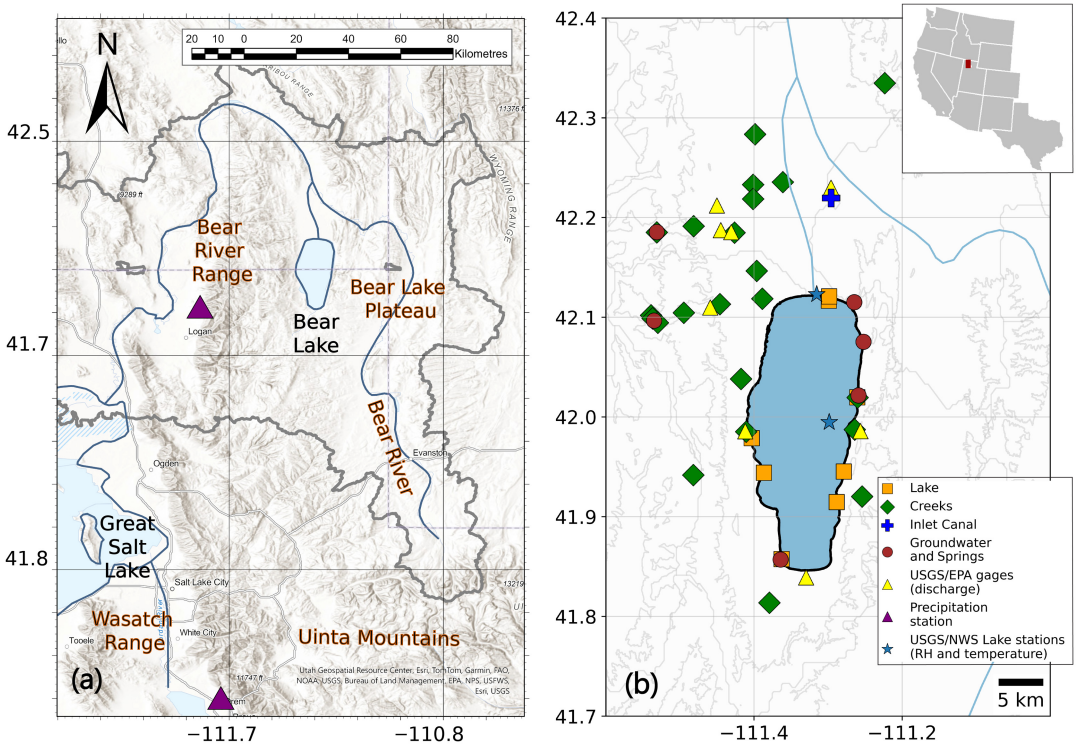

Figure 1 **(a)** Bear River watershed (grey outline) map and **(b)** sampling site locations; inset shows Bear Lake in the western U.S. This study utilised replicate samples from sites shown in panel **(b)** and previously reported by Custado *et al.* (2025).

Table 1 Comparison of calculated relative humidity and X_e. Values are reported as median and IQR from 100,000 Monte Carlo simulations due to the non-normality of the output distributions (Fig. S-2). Mean and 1σ values are in Table S-3.

Isotope system	Calculated *h* from Monte Carlo simulations*	Calculated *h* normalised to air temperature**	Evaporation/ Inflow (X_e)	Sample collection dates	References
Triple oxygen	0.590 *(IQR 0.375–0.774)*	0.532 *(IQR 0.338–0.698)*	0.267 *(IQR 0.231–0.308)*	August 2023	This study
$\delta^{18}O$-$\delta^{2}H$	0.639 *(IQR 0.455–0.788)*	0.577 *(IQR 0.411–0.711)*	0.281 *(IQR 0.240–0.321)*	August 2023	This study
$\delta^{18}O$-$\delta^{2}H$	0.62 ± 0.03	0.56 ± 0.03	0.38 ± 0.01	July 1981 to August 2023	Custado *et al.* (2025)

*Mass balance derived humidity is normalised to lake surface temperature, while instrument derived humidity is normalised to air temperature.
**Temperatures used for conversion: evaporation flux weighted lake (11.16 °C) and air temperature (12.72 °C). See Table S-4 for monthly values.

Isotopic Mass Balance of Bear Lake

Figure 2 illustrates our new isotopic data set in both $\delta'^{18}O$-$\Delta'^{17}O$ and $\delta^{18}O$-d-excess spaces, overlain on evaporation trajectories modelled as a function of X_e at different humidities (Eq. 1).

The volume weighted mean inflow (yellow star, Fig. 2) is composed of inputs from the inlet canal (orange diamond, 55.68 % of total volumetric inflow), on-lake precipitation (purple star, 18.91 %), creeks (orange star, 25.39 %), and groundwater (pink star, 0.01 %). The spread in the $\Delta'^{17}O$ of the inflow components, like d-excess, suggests potential for $\Delta'^{17}O$ to distinguish sources with different evaporation histories, as is the case with this system (inset plots, Fig. 2). For example, Voigt *et al.* (2021) previously demonstrated that $\Delta'^{17}O$ can resolve the evaporation trajectories of shallow lakes with and without recharge in Salar del Huasco, Chile. In contrast, Bear Lake is primarily fed by snowmelt from surrounding mountains, which exhibit a narrower range of d-excess values.

Deriving *h* and X_e from Mass Balance Calculations

Table 1 summarises the mass balance results along with the multi-year data set results of Custado *et al.* (2025).

The calculated uncertainties do not statistically differentiate the values in Table 1, partly due to the conservative approach used to generate input uncertainties, which better captures data variability (see Supplementary Information). Nevertheless, the median triple oxygen derived *h* and X_e are slightly lower than $\delta^{18}O$-$\delta^{2}H$ estimates and comparable to Custado *et al.* (2025). The observed discrepancies likely reflect temporal coverage differences in the data, while analytical uncertainty and data variability account for the modelled uncertainties (Table S-1).

The evaporation flux weighted relative humidity calculated from monthly United States Geological Survey (USGS) observations (Table S-4) is ~0.53, closer to the triple oxygen

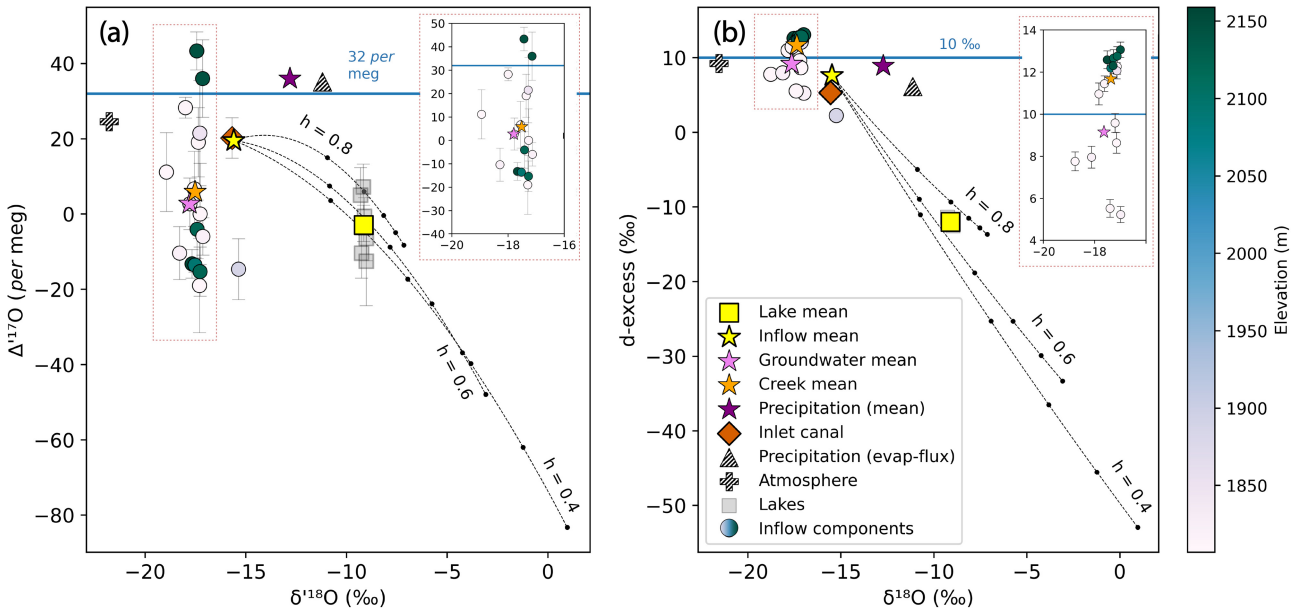

Figure 2 **(a)** $\Delta'^{17}O$ *versus* $\delta'^{18}O$ and **(b)** d-excess *versus* $\delta^{18}O$. Blue lines denote the Global Meteoric Water Line (GMWL), while black dashed lines represent lake isotopic evolution during evaporation at different humidities. Black dots indicate X_e values from 0 to 1 in increments of 0.2. Inflow components (circles) represent individual stream samples and are coloured by elevation; the inlet canal is included in the inflow mean. Insets show magnified views of the areas within the red dashed boxes. Only samples with paired discharge information were used in the calculations. Note that the error bars for d-excess are smaller than the markers. A link to the complete data set is included in the Supplementary Information.

derived median h when normalised to air temperature. This agreement suggests that triple oxygen data may better constrain above lake humidity, even with limited temporal resolution. Oxygen isotopes are generally more sensitive to kinetic fractionation than deuterium (Gonfiantini, 1986) and may therefore better record relative humidity changes. Additionally, the relative insensitivity of $\Delta'^{17}O$ to temperature compared to d-excess allows moisture source effects to be isolated without temperature corrections (Angert *et al.*, 2004; Uemura *et al.*, 2010). However, additional constraints on the input parameters are needed to reduce estimation errors.

Isotopic Controls on h and X_e

Previous studies have highlighted the sensitivity of isotopic mass balance models to varying isotopic and environmental inputs (*e.g.*, Gázquez *et al.*, 2018; Passey and Ji, 2019; Voigt *et al.*, 2021), particularly relative humidity and the isotopic compositions of inflow and atmospheric moisture (Barkan and Luz, 2007; Surma *et al.*, 2015, 2018; Voigt *et al.*, 2021). The influence of salinity and wind turbulence (n), while important, was not explicitly considered; instead a value of n = 0.5, commonly applied to lake studies (Gonfiantini, 1986; Criss, 1999; Gibson *et al.*, 2016), was adopted to correct for the α_{diff} values used (Table S-2). For this work, we focus on parameters that can be constrained given available environmental data. Nevertheless, we provide Figure S-3 to model the response of lake isotopic composition to varying n. Figure 3 summarises how lake isotopic composition, h, and X_e respond to a range of inputs.

In both systems, the spread in the modelled lake isotopic composition increases with X_e (Fig. 3a,b). This pattern is consistent when simulations are focused on separate input parameters, with humidity and isotopic composition of atmospheric moisture having the greatest relative influence at X_e = 1 (Fig. S-4). However, lake isotopic composition responds more strongly to inflow at lower X_e, likely due to less kinetic fractionation at lower evaporation rates (Fig. S-4a,e). Conversely, at higher X_e, the parameters that control the isotopic (δ_A) and moisture (h) gradient above the lake become increasingly important as more vapour escapes from the lake (Craig and Gordon, 1965).

Additionally, both isotope systems feature a triangular solution space for h and X_e (Fig. 3c), with the $\delta^{18}O$-δ^2H system showing greater divergence in X_e at higher h. Consequently, $\Delta'^{17}O$ appears to provide a tighter constraint on relative humidity and its trade off with X_e. Figure S-4 illustrates how this solution space changes when variability is isolated to individual parameters, showing that the spread at high h is primarily governed by δ_A (Fig. S-4). Despite preserving the GMWL relationship between atmospheric $\delta^{18}O$ with δ^2H in the model, the non-unique solutions at high h demonstrates the strong sensitivity of the $\delta^{18}O$-δ^2H system to atmospheric moisture variability.

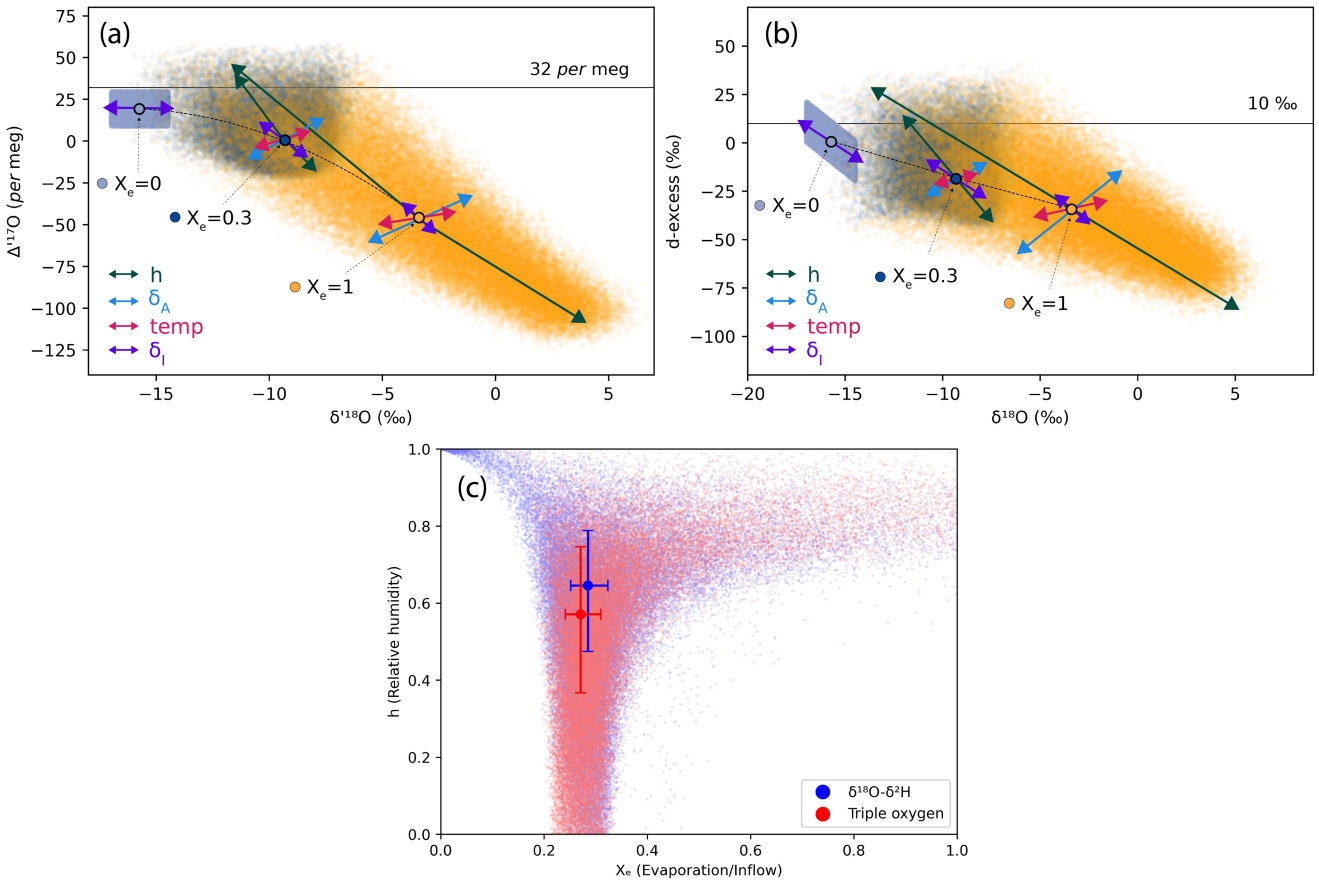

Figure 3 Sensitivity of lake isotopic composition and environmental parameters to varying evaporation conditions. Changes in the lake isotopic composition as a function of X_e are shown in **(a)** $\delta'^{18}O$ *versus* $\Delta'^{17}O$ and **(b)** $\delta^{18}O$ *versus* d-excess spaces, while changes in X_e (x axis) and h (y axis) from varying isotopic inputs are shown in **(c)**. Horizontal lines in **(a)** and **(b)** represent the GMWL. Error bars in **(c)** represent the IQR around the median value (circle). Inputs for **(a)** and **(b)** were h, δ_A, temperature, and δ_I; inputs for **(c)** were δ_A, temperature, δ_I, and lake composition (δ_L). Each marker represents one of 100,000 simulations sampled from normal distributions defined by the calculated input parameter values and uncertainties (see Supplementary Information). Arrows in **(a)** and **(b)** indicate the range of outputs generated by varying a single input while holding others constant (*cf.* Gázquez *et al.*, 2018). Corresponding individual simulations are compiled in Figure S-4.

Previous studies often rely on estimating δ_A due to difficulties in making direct measurements (Surma *et al.*, 2015, 2018; Gázquez *et al.*, 2018; Passey and Ji, 2019; Voigt *et al.*, 2021). Here, we estimated δ_A by assuming that atmospheric moisture upwind of the lake is in equilibrium with evaporation flux weighted mean precipitation, implicitly accounting for seasonality to better reproduce observed lake and inflow isotopic compositions (Eq. S-14; Gibson *et al.*, 2016; Custado *et al.*, 2025). Other studies instead assume complete or partial isotopic equilibrium between atmospheric moisture and inflow waters (Gázquez *et al.*, 2018; Passey and Ji, 2019), with limited existing measurements in continental settings (*e.g.*, Voigt *et al.*, 2021, 2025). Regardless of the chosen approach, fractionation during evaporation has been consistently demonstrated to be sensitive to both δ_A and relative humidity, underscoring the need for more direct measurements of these parameters.

Comparison to Previous Studies

To simulate palaeoclimate applications of $\Delta'^{17}O$ in lakes, we calculated the $\delta'^{17}O$-$\delta'^{18}O$ slope between the source and lake waters (λ_{lake}) using empirical λ_{lake}-$\Delta'^{17}O$ relationships derived by Passey and Ji (2019) and Katz *et al.* (2023), and subsequently, the reconstructed $\delta^{18}O$ of the unevaporated catchment precipitation ($\delta^{18}O_{rucp}$) (Eqs. S-15, S-16). Multiple λ_{lake}-$\delta^{18}O_{rucp}$ pairs were calculated from these empirical equations and compared with values derived directly from measured inflow and lake isotopic data. These values are summarised in Table S-5.

The calculated λ_{lake} values using the empirical coefficients (λ_{lake} = 0.5213 to 0.5235) yielded higher median $\delta^{18}O_{rucp}$ estimates (Table S-5) than the measured stream samples (−18.1 ± 1.4 ‰, Passey and Ji, 2019; −17.2 ± 0.6 ‰ (1σ), this study). In contrast, the λ_{lake} value calculated from measured inflow and lake samples (0.5246) resulted in a $\delta^{18}O_{rucp}$ value of −18.1 ± 5.4 ‰, expectedly lower than the measured stream samples. This discrepancy underscores the importance of additional data from diverse modern lake environments to refine empirical λ_{lake}-$\Delta'^{17}O$ relationships and better constrain inflow water distributions in palaeo-catchments.

Triple oxygen isotope mass balance models have been implemented in semi-permanent freshwater systems in arid environments, where groundwater recharge is of periodic importance (Surma *et al.*, 2015, 2018; Voigt *et al.*, 2021). These studies show that triple oxygen isotopes can distinguish between simple and recharged evaporation. Although Bear Lake currently receives minimal groundwater input, palaeoclimate records indicate that it has alternated between underfilled and overfilled states, implying periods of substantial groundwater influence (Bright, 2009; Dean, 2009; Kaufman *et al.*, 2009). Reconstructions of h and X_e from gypsum hydration waters where the lake balance model simultaneously solves for both isotope systems show that changes in X_e at higher values (>0.75) produce lower variations in the back calculated h (Gázquez *et al.*, 2018). Figure 3c shows that this observation is likely due to the constraints provided by the triple oxygen data. Together with the ability to reconstruct the isotopic composition of the unevaporated source waters, these observations demonstrate the potential of triple oxygen isotopes to provide unique hydrological insights.

Implications

Comparison of triple oxygen and $\delta^{18}O$-$\delta^{2}H$ isotopic systems reveals differing sensitivities to environmental and isotopic inputs when estimating h and X_e. Both systems yielded comparable X_e values, supporting their use in water management applications where quantifying hydrological balance components, such as evaporation, are essential (*e.g.*, Surma *et al.*, 2015; Custado *et al.*, 2025). Simultaneous use of both systems may best constrain multiple parametric unknowns (Gázquez *et al.*, 2018); however, improved monitoring of h and the isotopic composition of atmospheric moisture at the lake surface is necessary to reduce uncertainties in under constrained fluxes, such as evaporation and groundwater discharge, particularly in semi-arid regions where annual X_e values are typically high.

Additionally, patterns in our data suggest that $\Delta'^{17}O$ may be a more consistent recorder of above lake h. This finding supports the growing use of triple oxygen isotopes in palaeoclimate studies, which have been analysed in lacustrine carbonate and gypsum hydration waters to reconstruct past environmental conditions (Gázquez *et al.*, 2018; Passey and Ji, 2019; Katz *et al.*, 2023), and lacustrine chert to reconstruct past elevation (Ibarra *et al.*, 2021). However, mass balance derived h is normalised to lake temperature, making constraints on past lake temperatures important for palaeoclimate reconstructions. As shown in our calculations, even a modest difference between lake air temperatures yields considerably different h estimates (Table 1).

The combined use of $\Delta'^{17}O$ and d-excess has been proposed for tracking moisture sources, leveraging the lower temperature sensitivity of $\Delta'^{17}O$ relative to d-excess (Angert *et al.*, 2004; Uemura *et al.*, 2010). However, its application to reconstruct h and $\delta^{18}O_{rucp}$ requires well constrained isotopic inputs, as demonstrated by the differences between estimates derived from measured samples and empirical relationships. Therefore, this work underscores the need to expand $\Delta'^{17}O$ measurements of meteoric waters across seasons and environmental gradients to better characterise $\delta^{17}O$-$\delta^{18}O$ isotope system fractionation and improve accuracy of mass balance models and empirical relationships, such as those of Passey and Ji (2019) and Katz *et al.* (2023). Additionally, further improvements in analytical precision and throughput (*e.g.*, Hutchings and Konecky, 2023; Terzer-Wassmuth *et al.*, 2023) will also help reduce uncertainty.

Acknowledgements

This work was funded by NSF AGS 2102901 and AGS 2333-173 to DEI, NSF AGS 2333172 to JKCR, NSF AGS 2102884 to JLO, with additional support from the Brown University Division of Research.

Editor: Gavin Foster

Additional Information

Supplementary Information accompanies this letter at https://www.geochemicalperspectivesletters.org/article2631.

Cite this letter as: Custado, M.J., Waldeck, A.R., Belanger, B., Wang, X.-K., Rugenstein, J.C.K., Cobb, K.M., Oster, J.L., Ibarra, D.E. (2026) Contrasting controls on $\delta^{18}O$-$\delta^{2}H$ and

$\delta^{18}O$-$\delta^{17}O$ systematics in a balance filled lake. *Geochem. Persp. Let.* 41, 40–45. https://doi.org/10.7185/geochemlet.2631

References

Angert, A., Cappa, C.D., DePaolo, D.J. (2004) Kinetic ^{17}O effects in the hydrologic cycle: Indirect evidence and implications. *Geochimica et Cosmochimica Acta* 68, 3487–3495. https://doi.org/10.1016/j.gca.2004.02.010

Barkan, E., Luz, B. (2007) Diffusivity fractionations of $H_2^{16}O/H_2^{17}O$ and $H_2^{16}O/H_2^{18}O$ in air and their implications for isotope hydrology. *Rapid Communications in Mass Spectrometry* 21, 2999–3005. https://doi.org/10.1002/rcm.3180

Berman, E.S.F., Levin, N.E., Landais, A., Li, S., Owano, T. (2013) Measurement of $\delta^{18}O$, $\delta^{17}O$, and ^{17}O-excess in Water by Off-Axis Integrated Cavity Output Spectroscopy and Isotope Ratio Mass Spectrometry. *Analytical Chemistry* 85, 10392–10398. https://doi.org/10.1021/ac402366t

Bright, J. (2009) Isotope and major-ion chemistry of groundwater in Bear Lake Valley, Utah and Idaho, with emphasis on the Bear River Range. In: Rosenbaum, J.G., Kaufman, D.S. (Eds.) *Paleoenvironments of Bear Lake, Utah and Idaho, and its catchment*. Geological Society of America, Boulder, Special Paper 450, 105–132. https://doi.org/10.1130/2009.2450(04)

Craig, H., Gordon, L.I. (1965) Deuterium and oxygen 18 variations in the ocean and marine atmosphere. In: Tongiorgi, E. (Ed.) *Stable Isotopes in Oceanographic Studies and Paleotemperatures*. Spoleto, Italy, 9–130.

Criss, R.E. (1999) *Principles of Stable Isotope Distribution*. Oxford University Press, New York. https://doi.org/10.1093/oso/9780195117752.001.0001

Custado, M.J., Gagnon, C.A., Belanger, B., Sekhon, N., Bernstein-Schalet, J., Kinsley, C.W., Sharp, W.D., Oster, J.L., Ibarra, D.E. (2025) Constraining the Modern Hydrological Balance of Bear Lake, Utah-Idaho: Insights From Stable Isotopes ($\delta^{18}O$ and $\delta^{2}H$). *Water Resources Research* 61, e2024WR038264. https://doi.org/10.1029/2024WR038264

Dean, W.E. (2009) Endogenic carbonate sedimentation in Bear Lake, Utah and Idaho, over the last two glacial-interglacial cycles. In: Rosenbaum, J.G., Kaufman, D.S. (Eds.) *Paleoenvironments of Bear Lake, Utah and Idaho, and its catchment*. Geological Society of America, Boulder, Special Paper 450, 169–196. https://doi.org/10.1130/2009.2450(07)

Gat, J.R. (1995) Stable Isotopes of Fresh and Saline Lakes. In: Lerman, A., Imboden, D.M., Gat, J.R. (Eds.) *Physics and Chemistry of Lakes*. Second Edition, Springer, Berlin, Heidelberg, 139–165. https://doi.org/10.1007/978-3-642-85132-2_5

Gázquez, F., Morellón, M., Bauska, T., Herwartz, D., Surma, J., *et al.* (2018) Triple oxygen and hydrogen isotopes of gypsum hydration water for quantitative paleo-humidity reconstruction. *Earth and Planetary Science Letters* 481, 177–188. https://doi.org/10.1016/j.epsl.2017.10.020

Gázquez-Sánchez, F., Jiménez-Espejo, F., Rodríquez-Rodríquez, M., Martegani, L., Voigt, C., *et al.* (2023) Roman water management impacted the hydrological functioning of wetlands during drought periods. *Scientific Reports* 13, 18815. https://doi.org/10.1038/s41598-023-46010-5

Gibson, J.J., Birks, S.J., Yi, Y. (2016) Stable isotope mass balance of lakes: a contemporary perspective. *Quaternary Science Reviews* 131, 316–328. https://doi.org/10.1016/j.quascirev.2015.04.013

Gonfiantini, R. (1986) Environmental Isotopes in Lake Studies. In: Fritz, P., Fontes, J.Ch. (Eds.) *Handbook of Environmental Isotope Geochemistry: Volume 2, The Terrestrial Environment, B*. Elsevier, Amsterdam, 113–168. https://doi.org/10.1016/B978-0-444-42225-5.50008-5

Gröning, M. (2011) Improved water $\delta^{2}H$ and $\delta^{18}O$ calibration and calculation of measurement uncertainty using a simple software tool. *Rapid Communications in Mass Spectrometry* 25, 2711–2720. https://doi.org/10.1002/rcm.5074

Hutchings, J.A., Konecky, B.L. (2023) Optimization of a Picarro L2140-i cavity ring-down spectrometer for routine measurement of triple oxygen isotope ratios in meteoric waters. *Atmospheric Measurement Techniques* 16, 1663–1682. https://doi.org/10.5194/amt-16-1663-2023

Ibarra, D.E., Kukla, T., Methner, K.A., Mulch, A., Chamberlain, C.P. (2021) Reconstructing Past Elevations From Triple Oxygen Isotopes of Lacustrine Chert: Application to the Eocene Nevadaplano, Elko Basin, Nevada, United States. *Frontiers in Earth Science* 9, 628868. https://doi.org/10.3389/feart.2021.628868

Katz, S.A., Levin, N.E., Rodbell, D.T., Gillikin, D.P., Aron, P.G., Passey, B.H., Tapia, P.M., Serrepe, A.R., Abbott, M.B. (2023) Detecting hydrologic distinctions among Andean lakes using clumped and triple oxygen isotopes. *Earth and Planetary Science Letters* 602, 117927. https://doi.org/10.1016/j.epsl.2022.117927

Kaufman, D.S., Bright, J., Dean, W.E., Rosenbaum, J.G., Moser, K., *et al.* (2009) A quarter-million years of paleoenvironmental change at Bear Lake, Utah and Idaho. In: Rosenbaum, J.G., Kaufman, D.S. (Eds.) *Paleoenvironments of Bear Lake, Utah and Idaho, and its catchment.* Geological Society of America, Boulder, Special Paper 450, 311–351. https://doi.org/10.1130/2009.2450(14)

Luz, B., Barkan, E. (2010) Variations of $^{17}O/^{16}O$ and $^{18}O/^{16}O$ in meteoric waters. *Geochimica et Cosmochimica Acta* 74, 6276–6286. https://doi.org/10.1016/j.gca.2010.08.016

Miller, M.F. (2002) Isotopic fractionation and the quantification of ^{17}O anomalies in the oxygen three-isotope system: an appraisal and geochemical significance. *Geochimica et Cosmochimica Acta* 66, 1881–1889. https://doi.org/10.1016/S0016-7037(02)00832-3

Passey, B.H., Ji, H. (2019) Triple oxygen isotope signatures of evaporation in lake waters and carbonates: A case study from the western United States. *Earth and Planetary Science Letters* 518, 1–12. https://doi.org/10.1016/j.epsl.2019.04.026

Passey, B.H., Levin, N.E. (2021) Triple Oxygen Isotopes in Meteoric Waters, Carbonates, and Biological Apatites: Implications for Continental Paleoclimate Reconstruction. *Reviews in Mineralogy and Geochemistry* 86, 429–462. https://doi.org/10.2138/rmg.2021.86.13

Pierchala, A., Rozanski, K., Dulinski, M., Gorczyca, Z. (2022) Quantification the diffusion-induced fractionation of $^{1}H_2{}^{17}O$ isotopologue in air accompanying the process of water evaporation. *Geochimica et Cosmochimica Acta* 322, 244–259. https://doi.org/10.1016/j.gca.2022.01.020

Steig, E.J., Jones, T.R., Schauer, A.J., Kahle, E.C., Morris, V.A., Vaughn, B.H., Davidge, L., White, J.W.C. (2021) Continuous-Flow Analysis of $\delta^{17}O$, $\delta^{18}O$, and δD of H_2O on an Ice Core from the South Pole. *Frontiers in Earth Science* 9, 640292. https://doi.org/10.3389/feart.2021.640292

Surma, J., Assonov, S., Bolourchi, M.J., Staubwasser, M. (2015) Triple oxygen isotope signatures in evaporated water bodies from the Sistan Oasis, Iran. *Geophysical Research Letters* 42, 8456–8462. https://doi.org/10.1002/2015GL066475

Surma, J., Assonov, S., Herwartz, D., Voigt, C., Staubwasser, M. (2018) The evolution of ^{17}O-excess in surface water of the arid environment during recharge and evaporation. *Scientific Reports* 8, 4972. https://doi.org/10.1038/s41598-018-23151-6

Terzer-Wassmuth, S., Wassenaar, L.I., Araguás-Araguás, L.J., Stumpp, C. (2023) Balancing precision and throughput of $\delta^{17}O$ and $\Delta'^{17}O$ analysis of natural waters by Cavity Ringdown Spectroscopy. *MethodsX* 10, 102150. https://doi.org/10.1016/j.mex.2023.102150

Uemura, R., Barkan, E., Abe, O., Luz, B. (2010) Triple isotope composition of oxygen in atmospheric water vapor. *Geophysical Research Letters* 37, L04402. https://doi.org/10.1029/2009GL041960

Voigt, C., Herwartz, D., Dorador, C., Staubwasser, M. (2021) Triple oxygen isotope systematics of evaporation and mixing processes in a dynamic desert lake system. *Hydrology and Earth System Sciences* 25, 1211–1228. https://doi.org/10.5194/hess-25-1211-2021

Voigt, C., Gázquez, F., Martegani, L., Sánchez Villanueva, A.I., Medina, A., Jiménez-Espinosa, R., Jiménez-Millán, J., Rodríguez-Rodríguez, M. (2025) How seasonal hydroclimate variability drives the triple oxygen and hydrogen isotope composition of small lake systems in semiarid environments. *Hydrology and Earth System Sciences* 29, 1783–1806. https://doi.org/10.5194/hess-29-1783-2025